

An open-system quantum simulator with trapped ions

Julio T. Barreiro^{1*}, Markus Müller^{2,3*}, Philipp Schindler¹, Daniel Nigg¹, Thomas Monz¹, Michael Chwalla^{1,2}, Markus Hennrich¹, Christian F. Roos^{1,2}, Peter Zoller^{2,3} & Rainer Blatt^{1,2}

The control of quantum systems is of fundamental scientific interest and promises powerful applications and technologies. Impressive progress has been achieved in isolating quantum systems from the environment and coherently controlling their dynamics, as demonstrated by the creation and manipulation of entanglement in various physical systems. However, for open quantum systems, engineering the dynamics of many particles by a controlled coupling to an environment remains largely unexplored. Here we realize an experimental toolbox for simulating an open quantum system with up to five quantum bits (qubits). Using a quantum computing architecture with trapped ions, we combine multi-qubit gates with optical pumping to implement coherent operations and dissipative processes. We illustrate our ability to engineer the open-system dynamics through the dissipative preparation of entangled states, the simulation of coherent many-body spin interactions, and the quantum non-demolition measurement of multi-qubit observables. By adding controlled dissipation to coherent operations, this work offers novel prospects for open-system quantum simulation and computation.

Every quantum system is inevitably coupled to its surrounding environment. Significant progress has been made in isolating systems from their environment and coherently controlling the dynamics of several qubits^{1–4}. These achievements have enabled the realization of high-fidelity quantum gates and the implementation of small-scale quantum computing and communication devices, as well as the measurement-based probabilistic preparation of entangled states in atomic^{5,6}, photonic⁷, NMR⁸ and solid-state set-ups^{9–11}. In particular, successful demonstrations of quantum simulators^{12,13}, which allow one to mimic and study the dynamics of complex quantum systems, have been reported¹⁴.

In contrast, controlling the more general dynamics of open systems amounts to engineering both the Hamiltonian time evolution of the system as well as the coupling to the environment. In previous work^{15–18}, controlled decoherence has been used to systematically study the detrimental effects of decoherence on many-body or multi-qubit open systems. The ability to design dissipation can, however, be a useful resource, as in the context of the preparation of a desired entangled state from an arbitrary initial state^{19–21}, and in the closely related fields of dissipative quantum computation²² and quantum memories²³. It also enables the preparation and manipulation of many-body states and quantum phases²⁰, and provides an enhanced sensitivity in precision measurements²⁴. In particular, by combining suitably chosen coherent and dissipative operations, one can engineer the system–environment coupling, thus generalizing the concept of Hamiltonian quantum simulation to open quantum systems^{13,25}.

Here we provide an experimental demonstration of a toolbox of coherent and dissipative multi-qubit manipulations to control the dynamics of open systems. In a string of trapped ions, each ion encoding a qubit, we subdivide the qubits into ‘system’ and ‘environment’. The system–environment coupling is then engineered through the universal set of quantum operations available in ion-trap quantum computers^{26,27}, whereas the environment ion is coupled to

the dissipative bath of vacuum modes of the radiation field via optical pumping. Following ref. 22 (see also ref. 28), these quantum resources provide a complete toolbox to engineer general Markovian open-system dynamics in our multi-qubit system^{25,29}.

We first illustrate this engineering by dissipatively preparing a Bell state in a 2+1 ion system (that is, two system ions and one ancilla ion), such that an initially fully mixed state is pumped into a given Bell state. Similarly, with 4+1 ions, we also dissipatively prepare a four-qubit Greenberger–Horne–Zeiling (GHZ) state, which can be regarded as a minimal instance of Kitaev’s toric code³⁰. Besides the dissipative elements, we show coherent *n*-body interactions by implementing the fundamental building block for four-spin interactions. In addition, we demonstrate a readout of *n*-particle observables in a non-destructive way with a quantum-non-demolition (QND) measurement of a four-qubit stabilizer operator. We conclude by outlining future perspectives and implications of the present work for quantum information processing and simulation, as well as open-system quantum control scenarios including feedback²⁵.

Open-system dynamics and Bell-state pumping

The dynamics of an open quantum system *S* coupled to an environment *E* can be described by the unitary transformation $\rho_{SE} \mapsto U \rho_{SE} U^\dagger$, with ρ_{SE} the joint density matrix of the composite system *S* + *E*. Thus, the reduced density operator of the system will evolve as $\rho_S = \text{Tr}_E(U \rho_{SE} U^\dagger)$. The time evolution of the system can also be described by a completely positive Kraus map

$$\rho_S \mapsto \mathcal{E}(\rho_S) = \sum_k E_k \rho_S E_k^\dagger \quad (1)$$

with E_k operation elements satisfying $\sum_k E_k^\dagger E_k = 1$, and initially uncorrelated system and environment³¹. If the system is decoupled from the environment, the general map (1) reduces to $\rho_S \mapsto U_S \rho_S U_S^\dagger$, with U_S the unitary time evolution operator acting only on the system.

¹Institut für Experimentalphysik, Universität Innsbruck, Technikerstrasse 25, 6020 Innsbruck, Austria. ²Institut für Quantenoptik und Quanteninformation, Österreichische Akademie der Wissenschaften, Technikerstrasse 21A, 6020 Innsbruck, Austria. ³Institut für Theoretische Physik, Universität Innsbruck, Technikerstrasse 25, 6020 Innsbruck, Austria.

*These authors contributed equally to this work.

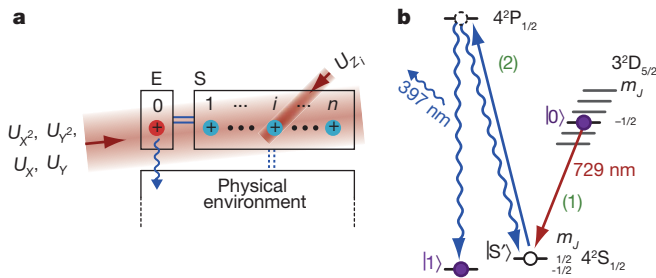


Figure 1 | Experimental tools for the simulation of open quantum systems with ions. **a**, The coherent component is realized by collective ($U_X, U_Y, U_{X^2}, U_{Y^2}$) and single-qubit operations (U_Z) on a string of $^{40}\text{Ca}^+$ ions which consists of the environment qubit (ion 0) and the system qubits (ions 1 to n). Coherent operations on S and E, combined with a controllable dissipative mechanism involving spontaneous emission of a photon from the environment ion, allow one to tailor the coupling of the system qubits to an artificial environment. This should be contrasted to the residual, detrimental coupling of the system (and environment) ions to their physical environment. **b**, The dissipative mechanism on the ancilla qubit is realized in the two steps shown on the Zeeman-split $^{40}\text{Ca}^+$ levels by (1) a coherent transfer of the population from $|0\rangle$ to $|S'\rangle$ (brown arrow) and (2) an optical pumping to $|1\rangle$ after a transfer to the $4^2P_{1/2}$ state by a circularly-polarized laser at 397 nm (represented by a blue straight arrow).

Control of both coherent and dissipative dynamics is then achieved by finding corresponding sequences of maps (1) specified by sets of operation elements $\{E_k\}$ and engineering these sequences in the laboratory. In particular, for the example of dissipative quantum-state preparation, pumping to an entangled state $|\psi\rangle$ reduces to implementing appropriate sequences of dissipative maps. These maps are chosen to drive the system to the desired target state irrespective of its initial state. The resulting dynamics have then the pure state $|\psi\rangle$ as the unique attractor, $\rho_S \rightarrow |\psi\rangle\langle\psi|$. In quantum optics and atomic physics, the techniques of optical pumping and laser cooling are successfully used for the dissipative preparation of quantum states, although on a single-particle level. The engineering of dissipative maps for the preparation of entangled states can be seen as a generalization of this concept of pumping and cooling in driven dissipative systems to a many-particle context. To be concrete, we focus on dissipative preparation of stabilizer states, which represent a large family of entangled states, including graph states and error-correcting codes³².

We start by outlining the concept of Kraus map engineering for the simplest non-trivial example of ‘pumping’ a system of two qubits into a Bell state. The Hilbert space of two qubits is spanned by the four Bell states defined as $|\Phi^\pm\rangle = \frac{1}{\sqrt{2}}(|00\rangle \pm |11\rangle)$ and $|\Psi^\pm\rangle = \frac{1}{\sqrt{2}}(|01\rangle \pm |10\rangle)$. Here, $|0\rangle$ and $|1\rangle$ denote the computational basis of each qubit, and we use the short-hand notation $|00\rangle = |0\rangle_1|0\rangle_2$, for example. These maximally entangled states are stabilizer states: the Bell state $|\Phi^+\rangle$, for instance, is said to be stabilized by the two stabilizer operators Z_1Z_2 and X_1X_2 , where X and Z denote the usual Pauli matrices, as it is the only two-qubit state that is an eigenstate of eigenvalue $+1$ of these two commuting observables, that is, $Z_1Z_2|\Phi^+\rangle = |\Phi^+\rangle$ and $X_1X_2|\Phi^+\rangle = |\Phi^+\rangle$. In fact, each of the four Bell states is uniquely determined as an eigenstate with eigenvalues ± 1 with respect to Z_1Z_2 and X_1X_2 . The key idea of pumping is that we can achieve dissipative dynamics which pump the system into a particular Bell state, for example $\rho_S \rightarrow |\Psi^-\rangle\langle\Psi^-|$, by constructing two dissipative maps, under which the two qubits are irreversibly transferred from the $+1$ into the -1 eigenspaces of Z_1Z_2 and X_1X_2 .

The dissipative maps are engineered with the aid of an ancilla ‘environment’ qubit^{25,33} and a quantum circuit of coherent and dissipative operations. The form and decomposition of these maps into basic operations are discussed in Box 1. The pumping dynamics are determined by the probability of pumping from the $+1$ into the -1 stabilizer eigenspaces, which can be directly controlled by varying the parameters in the employed gate operations. For pumping with unit probability ($p = 1$), the two qubits reach the target Bell state—regardless of their initial state—after only one pumping cycle, that is, by a single application

of each of the two maps. In contrast, when the pumping probability is small ($p \ll 1$), the process can be regarded as the infinitesimal limit of the general map (1). In this case, the system dynamics under a repeated application of the pumping cycle are described by a master equation³⁴:

$$\dot{\rho}_S = -i[H_S, \rho_S] + \sum_k \left(c_k \rho_S c_k^\dagger - \frac{1}{2} c_k^\dagger c_k \rho_S - \rho_S \frac{1}{2} c_k^\dagger c_k \right) \quad (2)$$

Here H_S is a system Hamiltonian, and c_k are Lindblad operators reflecting the system–environment coupling. For the purely dissipative maps discussed here, $H_S = 0$. Quantum jumps from the $+1$ into the -1 eigenspace of Z_1Z_2 and X_1X_2 are mediated by a set of two-qubit Lindblad operators (see Box 1 for details); here the system reaches the target Bell state asymptotically after many pumping cycles.

Experimental Bell-state pumping

The dissipative preparation of n -particle entangled states is realized in a system of $n + 1$ $^{40}\text{Ca}^+$ ions confined to a string by a linear Paul trap and cooled to the ground state of the axial centre-of-mass mode³⁵. For each ion, the internal electronic Zeeman levels $D_{5/2}(m = -1/2)$ and $S_{1/2}(m = -1/2)$ encode the logical states $|0\rangle$ and $|1\rangle$ of a qubit. For coherent operations, a laser at a wavelength of 729 nm excites the quadrupole transition connecting the qubit states ($S_{1/2} \leftrightarrow D_{5/2}$). A broad beam of this laser couples to all ions (Fig. 1a) and realizes the collective single-qubit gate $U_X(\theta) = \exp(-i\frac{\theta}{2}\sum_i X_i)$ as well as a Mølmer-Sørensen³⁶ (MS) entangling operation $U_{X^2}(\theta) = \exp(-i\frac{\theta}{4}(\sum_i X_i)^2)$ when using a bichromatic light field (θ is controlled by the intensity and length of the laser pulses). Shifting the optical phase of the drive field by $\pi/2$ exchanges X_i by Y_i in these operations. As a figure of merit of our entangling operation, we can prepare 3 (5) qubits in a GHZ state with 98% (95%) fidelity³⁷. These collective operations form a universal set of gates when used in conjunction with single-qubit rotations $U_{Z_i}(\theta) = \exp(-i\frac{\theta}{2}Z_i)$, which are realized by an off-resonant laser beam that can be adjusted to focus on any ion.

For engineering dissipation, the key element of the mapping steps, shown as (i) and (iii) in Box 1, is a single MS operation. The two-qubit gate, step (ii), is realized by a combination of collective and single-qubit operations. The dissipative mechanism, step (iv), is here carried out on the ancilla qubit by a reinitialization into $|1\rangle$, as shown in Fig. 1b. Another dissipative process (P.S. *et al.*, manuscript in preparation) can be used to prepare the system qubits in a completely mixed state by the transfer $|0\rangle \rightarrow (|0\rangle + |S'\rangle)/\sqrt{2}$ followed by optical pumping of $|S'\rangle$ into $|1\rangle$, where $|S'\rangle$ is the electronic level $S_{1/2}(m = 1/2)$.

Qubit read-out is accomplished by fluorescence detection on the $S_{1/2} \leftrightarrow P_{1/2}$ transition. The ancilla qubit can be measured without affecting the system qubits by applying hiding pulses that shelve the system qubits in the $D_{5/2}$ state manifold during fluorescence detection³⁸.

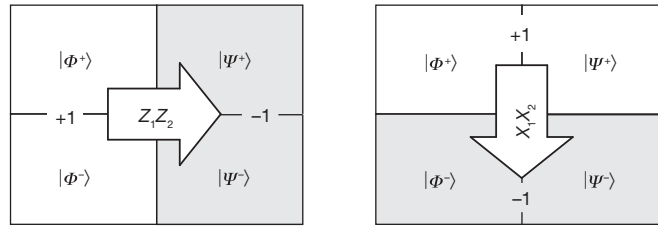
We use these tools to implement up to three Bell-state pumping cycles on a string of $2 + 1$ ions. Starting with the two system qubits in a completely mixed state, we pump towards the Bell state $|\Psi^-\rangle$. Each pumping cycle is accomplished with a sequence of eight entangling operations, four collective unitaries and six single-qubit operations (see Supplementary Information). The pumping dynamics are probed by quantum state tomography of the system qubits after every half cycle. The reconstructed states are then used to map the evolution of the Bell-state populations.

In a first experiment, we set the pumping probability at $p = 1$ to observe deterministic pumping, and we obtain the Bell-state populations shown in Fig. 2a. As expected, the system reaches the target state after the first pumping cycle. Regardless of experimental imperfections, the target state population is preserved under the repeated application of further pumping cycles and reaches up to 91(1)% (all numbers in parentheses denote 1σ confidence intervals) after 1.5

BOX 1

Engineering dissipative open-system dynamics

Dissipative dynamics that pump two qubits from an arbitrary initial state into the Bell state $|\Psi^-\rangle$ are realized by two maps that generate pumping from the +1 into the -1 eigenspaces of the stabilizer operators Z_1Z_2 and X_1X_2 :



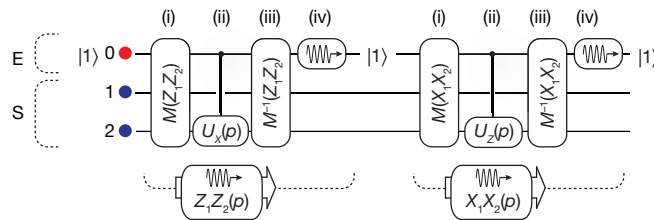
For Z_1Z_2 , the dissipative map pumping into the -1 eigenspace is $\rho_S \mapsto \mathcal{E}(\rho_S) = E_1 \rho_S E_1^\dagger + E_2 \rho_S E_2^\dagger$ with

$$E_1 = \sqrt{\rho} X_2 \frac{1}{2} (1 + Z_1 Z_2)$$

$$E_2 = \frac{1}{2} (1 - Z_1 Z_2) + \sqrt{1 - \rho} \frac{1}{2} (1 + Z_1 Z_2)$$

The map's action as a unidirectional pumping process can be seen as follows. As the operation element E_1 contains the projector $\frac{1}{2}(1 + Z_1Z_2)$ onto the +1 eigenspace of Z_1Z_2 , the spin flip X_2 can then convert +1 into -1 eigenstates of Z_1Z_2 ; for example, $|\Phi^+\rangle \mapsto |\Psi^+\rangle$. In contrast, the -1 eigenspace of Z_1Z_2 is left invariant. In the limit $\rho \ll 1$, the repeated application of this map reduces the process to a master equation with Lindblad operator $c = \frac{1}{2} X_2 (1 + Z_1 Z_2)$.

We implement the two dissipative maps by quantum circuits of three unitary operations (i)–(iii) and a dissipative step (iv). Both maps act on the two system qubits S and an ancilla which plays the role of the environment E .

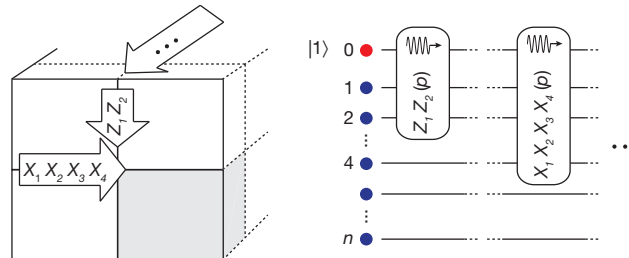


Pumping Z_1Z_2 proceeds as follows: (i) Information about whether the system is in the +1 or -1 eigenspace of Z_1Z_2 is mapped by $M(Z_1Z_2)$ onto the logical states $|0\rangle$ and $|1\rangle$ of the ancilla (initially in $|1\rangle$). (ii) A controlled gate $C(p)$ converts +1 into -1 eigenstates by flipping the state of the second qubit with probability p , where

$$C(p) = |0\rangle\langle 0|_0 \otimes U_{X_2}(p) + |1\rangle\langle 1|_0 \otimes 1$$

with $U_{X_2}(p) = \exp(i\alpha X_2)$ and α controlling the pumping probability $p = \sin^2 \alpha$. (iii) The initial mapping is inverted by $M^{-1}(Z_1Z_2)$. At this stage, in general, the ancilla and system qubits are entangled. (iv) The ancilla is dissipatively reset to $|1\rangle$, which carries away entropy to 'cool' the two system qubits. The second map for pumping into the -1 eigenspace of X_1X_2 is obtained from interchanging the roles of X and Z above.

The engineering of dissipative maps can be readily generalized to systems of more qubits. As an example, dissipative preparation of n -qubit stabilizer states can be realized by a sequence of n dissipative maps (for example, for Z_1Z_2 and $X_1X_2X_3X_4$ pumping), which are implemented in analogy to the quantum circuits for Bell state pumping discussed above.



cycles (ideally 100%). In a second experiment, aimed at simulating master-equation dynamics, the probability is set at $p = 0.5$ to probe probabilistic pumping dynamics. The target state is then approached asymptotically (Fig. 2b). After pumping the system for three cycles with $p = 0.5$, up to 73(1)% of the initially mixed population is pumped into the target state (ideally 88%). To achieve Bell-state pumping in the limit of $p \ll 1$, the gate fidelities need to be raised closer to one because close to the stationary state of the dynamics, the pumping probability p per step for populating the target state competes directly

with loss processes at a rate ϵ . Such losses are associated with gate errors and lead to a steady state loss of fidelity that scales as $\propto \epsilon/p$ (see Supplementary Information for further details).

In order to completely characterize the Bell-state pumping process, we also perform a quantum process tomography³¹. As an example, the reconstructed process matrix for $p = 1$ after 1.5 cycles (Fig. 2c) has a Jamiolkowski process fidelity³⁹ of 87.0(7)% with the ideal dissipative process $\rho_S \mapsto |\Psi^-\rangle\langle\Psi^-|$ which maps an arbitrary state of the system into the Bell state $|\Psi^-\rangle$.

Four-qubit stabilizer pumping

The engineering of the system–environment coupling, as demonstrated by Bell-state pumping above, can be readily extended to larger n -qubit open quantum systems. We illustrate such an engineering experimentally with the dissipative preparation of a four-qubit GHZ state $(|0000\rangle + |1111\rangle)/\sqrt{2}$. This state is uniquely characterized as the simultaneous eigenstate of the four stabilizers Z_1Z_2, Z_2Z_3, Z_3Z_4 and $X_1X_2X_3X_4$, all with eigenvalue $+1$ (Fig. 3a). Therefore, the pumping dynamics into the GHZ state are realized by four consecutive dissipative steps, each pumping the system into the $+1$ eigenspaces of the four stabilizers. In a system of $4+1$ ions, we implement such pumping dynamics in a manner analogous to the Bell-state pumping sequence. Here, however, the circuit decomposition of one pumping cycle involves 16 five-ion entangling operations, 20 collective unitaries and 34 single-qubit operations; further details are given in Supplementary Information.

In order to observe this deterministic pumping process into the GHZ state, we begin by preparing the system ions in a completely mixed state. The evolution of the state of the system after each pumping step is characterized by quantum state tomography. The reconstructed density matrices shown in Fig. 3b for the initial and subsequent states arising in each step have a fidelity (in %), or state overlap⁴⁰, with the expected states of $\{79(2), 89(1), 79.7(7), 70.0(7), 55.8(4)\}$ (the final state is genuinely multi-partite entangled⁴¹); see Supplementary Information for further details. The pumping dynamics is clearly reflected by the measured expectation values of the stabilizers Z_iZ_j ($ij = 12, 23, 34, 14$) and $X_1X_2X_3X_4$ at each step, as shown in Fig. 3c.

Although the simulation of a master equation strictly requires small pumping probabilities, we perform an exploratory study as follows. We implement up to five consecutive $X_1X_2X_3X_4$ -stabilizer pumping steps with two probabilities $p = 1$ and 0.5 , for the initial state $|1111\rangle$. The measured expectation values of all relevant stabilizers for pumping with $p = 1$ are shown in Fig. 3d. After the first step, the stabilizer $X_1X_2X_3X_4$ reaches an expectation value of $-0.68(1)$; after the second step and up to the fifth step, it is preserved at $-0.72(1)$ regardless of experimental imperfections.

For $X_1X_2X_3X_4$ -stabilizer pumping with $p = 0.5$, the four-qubit expectation value increases at each step and asymptotically approaches $-0.54(1)$ (ideally -1 ; fit shown in Fig. 3d). A state tomography after

each pumping step yields fidelities (in %) with the expected GHZ state of $\{53(1), 50(1), 49(1), 44(1), 41(1)\}$. From the reconstructed density matrices, we determine that the states generated after one to three cycles are genuinely multi-partite entangled⁴¹.

Coherent four-particle interactions

The coupling of the system to an ancilla particle, as used above for the engineering of dissipative dynamics, can also be harnessed to mediate effective coherent n -body interactions between the system qubits^{31,33}. The demonstration of a toolbox for open-system quantum simulation is thus complemented by adding unitary maps $\rho_S \mapsto U_S \rho_S U_S^\dagger$ to the dissipative elements described above. Here, $U_S = \exp(-i\tau H_S)$ is the unitary time evolution operator for a time step τ , which is generated by a system Hamiltonian H_S . In contrast to the recent achievements^{42,43} of small-scale analogue quantum simulators based on trapped ions, where two-body spin Hamiltonians have been engineered directly⁴⁴, here we pursue a gate-based implementation following the concept of Lloyd’s digital quantum simulator¹³, where the time evolution is decomposed into a sequence of coherent (and dissipative) steps.

In particular, the available gate operations enable a simulation of n -body spin interactions, which we illustrate by implementing time dynamics of a four-body Hamiltonian $H_S = -gX_1X_2X_3X_4$. This example is motivated by the efforts to experimentally realize Kitaev’s toric code Hamiltonian³⁰, which is a sum of commuting four-qubit stabilizer operators representing four-body spin interactions. This paradigmatic model belongs to a whole class of spin systems, which have been discussed in the context of topological quantum computing and quantum phases exhibiting topological order⁴⁵.

The elementary unitary operation U_S can be realized in three steps by the circuit shown in Fig. 4a. (i) As in the stabilizer pumping above, an operation $M(X_1X_2X_3X_4)$, here realized by an entangling MS gate $U_{X^2}(\pi/2)$, coherently maps the information about whether the four system spins are in the $+1(-1)$ eigenspace of $X_1X_2X_3X_4$ onto the internal states $|0\rangle$ and $|1\rangle$ of the ancilla qubit. (ii) Owing to this mapping, effectively all $+1(-1)$ eigenstates acquire a phase $\beta/2(-\beta/2)$ by a subsequent single-qubit rotation $U_Z(\beta)$ on the ancilla ion. The simulation time step τ is related to the phase by $\beta = 2g\tau$. (iii) After the initial mapping is inverted by a second MS gate $U_{X^2}(\pi/2)$, the ancilla qubit returns to its initial state and decouples from the four system qubits,

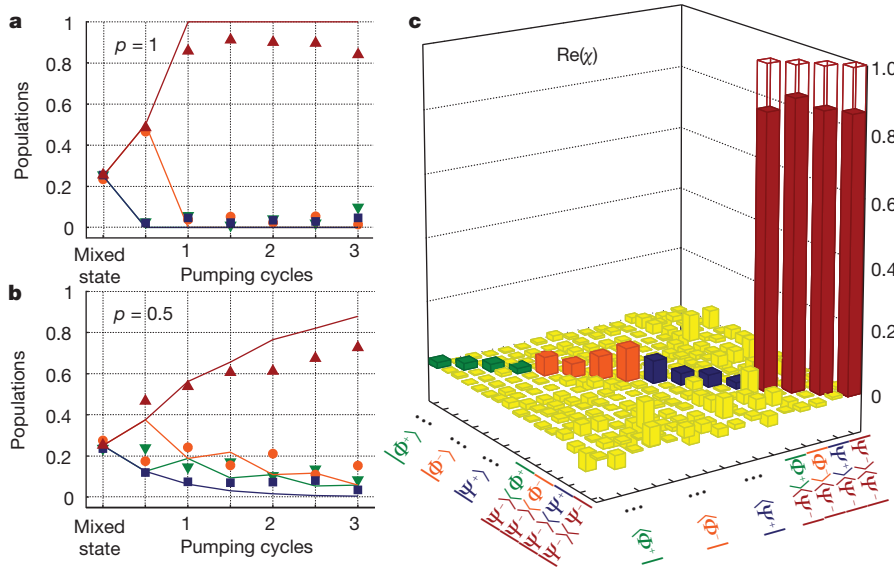


Figure 2 | Experimental signatures of Bell-state pumping. **a, b**, Evolution of the Bell-state populations $|\Phi^+\rangle$ (green down triangles), $|\Phi^-\rangle$ (orange circles), $|\Psi^+\rangle$ (blue squares) and $|\Psi^-\rangle$ (red up triangles) of an initially mixed state under a pumping process with probability $p = 1$ or deterministic (**a**) and $p = 0.5$ (**b**). Error bars, not shown, are smaller than 2% (1σ). **c**, Reconstructed process matrix χ (real part), displayed in the Bell-state basis, describing the

deterministic pumping of the two ions after one-and-a-half cycles. The ideal process mapping any input state into the state $|\Psi^-\rangle$ has as non-zero elements only the four transparent bars shown. The imaginary elements of χ , ideally all zero, have an average magnitude of 0.004 and a maximum of 0.03. The uncertainties in the elements of the process matrix are smaller than 0.01 (1σ). The colours of tickmarks and bars follow the colours used in **a** and **b**.

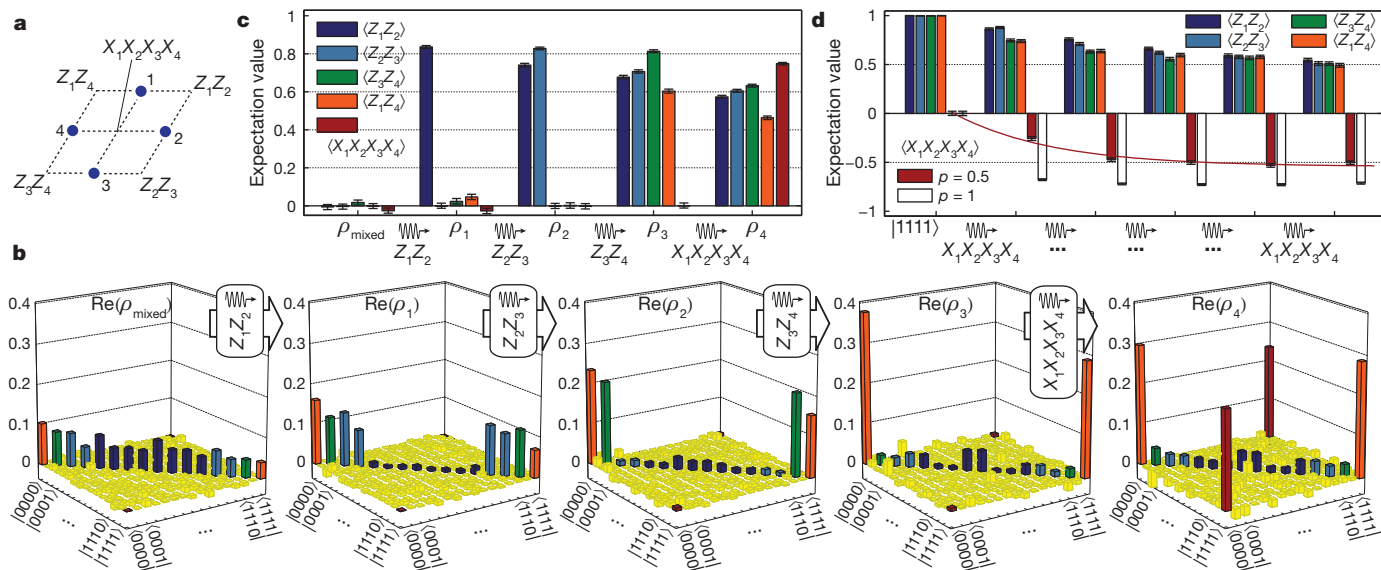


Figure 3 | Experimental signatures of four-qubit stabilizer pumping. **a**, Diagram of the four system qubits to be pumped into the GHZ state $(|0000\rangle + |1111\rangle)/\sqrt{2}$, which is uniquely characterized as the simultaneous eigenstate with eigenvalue +1 of the shown stabilizers. **b**, Reconstructed density matrices (real part) of the initial mixed state ρ_{mixed} and subsequent states $\rho_{1,2,3,4}$ after sequentially pumping the stabilizers Z_1Z_2 , Z_2Z_3 , Z_3Z_4 and $X_1X_2X_3X_4$. Populations in the initial mixed state with qubits i and j antiparallel, or in the -1 eigenspace of the Z_iZ_j stabilizer, disappear after pumping this stabilizer into the $+1$ eigenspace. For example, populations in dark blue disappear after Z_1Z_2 -stabilizer pumping. A final pumping of the stabilizer $X_1X_2X_3X_4$ builds up the

which in turn have evolved according to U_S . This compact sequence makes the simulation of n -body interactions experimentally efficient. Here, the use of global MS gates conveniently bundles the effect of several operations (M.M., K. Hammerer, Y. Zhou, C.F.R. and P.Z., manuscript in preparation) which arise in alternative circuit decompositions based on two-qubit gates³¹.

In an experiment carried out with 4+1 ions, we apply U_S for different values of τ to the system ions initially prepared in $|1111\rangle$. We observe coherent oscillations in the subspace spanned by $|0000\rangle$ and $|1111\rangle$, as shown in Fig. 4b. We characterize our implementation of U_S by comparing the expected and measured states, determined by quantum state tomography, for each value of τ . The fidelity between the expected and measured states is on average 85(2)%.

QND measurement of a four-qubit stabilizer

Our toolbox for quantum simulation of open systems is extended by the possibility of reading out n -body observables in a non-destructive

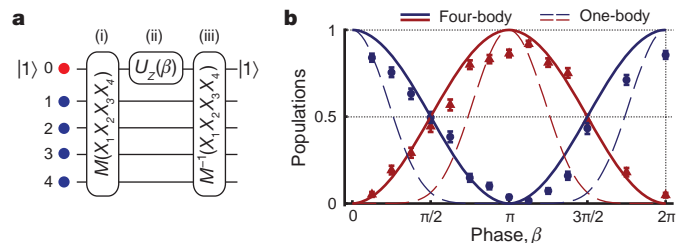


Figure 4 | Coherent simulation of four-body spin interactions. **a**, The elementary building block for the simulation of coherent evolution $U_S = \exp(-i\tau H_S)$ corresponding to the four-body Hamiltonian $H_S = -gX_1X_2X_3X_4$ ($\beta = 2g\tau$). **b**, Experimentally measured populations in state $|0000\rangle$ (up triangles) and $|1111\rangle$ (circles) as a function of β for a single application of U_S to the initial state $|1111\rangle$ of the four system qubits (error bars, $\pm 1\sigma$). The solid lines show the ideal behaviour. For comparison, the dashed lines indicate these populations for simultaneous single-qubit (one-body) oscillations, each driven by the rotation $\exp(-i\frac{\beta}{2}X_i)$.

coherence between $|0000\rangle$ and $|1111\rangle$, shown as red bars in the density matrix of ρ_4 . **c**, Measured expectation values of the relevant stabilizers; ideally, non-zero expectation values have a value of +1. **d**, Evolution of the measured expectation values of the relevant stabilizers for repeatedly pumping an initial state $|1111\rangle$ with probability $p = 0.5$ into the -1 eigenspace of the stabilizer $X_1X_2X_3X_4$. The incremental pumping is evident by the red line fitted to the pumped stabilizer expectation value. The evolution of the expectation value $\langle X_1X_2X_3X_4 \rangle$ for deterministic pumping ($p = 1$) is also shown. The observed decay of $\langle Z_iZ_j \rangle$ is due to imperfections and is detrimental to the pumping process (see Supplementary Information). Error bars (**c** and **d**), $\pm 1\sigma$.

way, which is also an essential ingredient in quantum error correction protocols. Here, we illustrate this for a four-qubit stabilizer operator $X_1X_2X_3X_4$. As above, we first coherently map the information about whether the system spins are in the $+1$ (-1) eigenspace of the stabilizer operator onto the logical states $|0\rangle$ and $|1\rangle$ of the ancilla qubit. In contrast to the engineering of coherent and dissipative maps above, where this step was followed by single- and two-qubit gate operations, here we proceed instead by measuring the ancilla qubit.

Thus, depending on the measurement outcome for the ancilla, the system qubits are projected onto the corresponding eigenspace of the stabilizer: $\rho_S \mapsto P_{\pm} \rho_S P_{\pm} / N_{\pm}$ ($P_{\pm} = \rho_S P_{\pm} / N_{\pm}$) for finding the ancilla in $|0\rangle$ ($|1\rangle$) with the normalization factor $N_{\pm} = \text{Tr}(P_{\pm} \rho_S P_{\pm})$. Here, $P_{\pm} = \frac{1}{2}(1 \pm X_1X_2X_3X_4)$ denote the projectors onto the ± 1 eigenspaces of the stabilizer operator. Note that our measurement is QND in the sense that (superposition) states within one of the two eigenspaces are not affected by the measurement.

In the experiment with 4+1 ions, we prepare different four-qubit system input states (tomographically characterized in additional experiments), carry out the QND measurement and tomographically determine the resulting system output states.

To characterize how well the measurement device prepares a definite state, we use as input $|1111\rangle$, which is a non-eigenstate of the stabilizer. In this case, when the ancilla qubit is found in $|0\rangle$ or $|1\rangle$ the system qubits are prepared in the state $(|0000\rangle \pm |1111\rangle)/\sqrt{2}$ by the QND measurement. Experimentally we observe this behaviour with a quantum state preparation (QSP) fidelity⁴⁶ of $F_{\text{QSP}} = 73(1)\%$. On the other hand, for a stabilizer eigenstate, the QND measurement preserves the stabilizer expectation value. Experimentally, for the input state $(|0011\rangle - |1100\rangle)/\sqrt{2}$, we observe a QND fidelity⁴⁶ of $F_{\text{QND}} = 96.9(6)\%$. For more details, see Supplementary Information.

Conclusions and outlook

In the present work, we have demonstrated engineering of dissipative Kraus maps for Bell-state and four-qubit stabilizer pumping. These particular examples exploited the available quantum resources by

coupling the system qubits to an ancilla by a universal set of entangling operations. The engineered environment was here represented by an ancilla ion undergoing optical pumping by dissipative coupling to the vacuum modes of the radiation field. These experiments, where the ancilla remains unobserved, represent an open-loop dynamics. Such scenarios were recently discussed in the context of an open-system quantum simulator for spin models, including lattice gauge theories, realized with Rydberg atoms in optical lattices. In fact, four-qubit stabilizer pumping together with four-spin interactions demonstrate the basic ingredients²⁸ for the simulation of spin dynamics and ground-state cooling for Kitaev's toric code Hamiltonian³⁰ on a single four-spin plaquette.

For a closed system, only a small number of Hamiltonians as generators are required to generate all possible unitary time evolutions. In the context of qubits, this is given by a finite set of single qubit operations together with an entangling CNOT gate. In contrast, as noted in refs 25 and 29, when a single ancilla qubit is used, the most general Markovian open-system dynamics cannot be obtained with a finite set of non-unitary open-loop transformations. However, such a universal dynamical control can be achieved through repeated application of coherent control operations and measurement of the ancilla qubit, followed by classical feedback operations onto the system. We note that our demonstration of a multi-qubit QND measurement provides, in combination with our previously demonstrated feedback techniques⁴⁷, the basic ingredient for the realization of such closed-loop dynamics.

Our experimental demonstration of a toolbox of elementary building blocks in a system of trapped ions should be seen as a conceptual step towards the realization of an open quantum system simulator with applications in various fields¹⁴, including condensed-matter physics and quantum chemistry, possibly in modelling quantum effects in biology⁴⁸, and in quantum computation driven by dissipation²².

Although the present experiments were performed with a linear ion-trap quantum computer architecture, the continuing development of two-dimensional trap arrays promises scalable implementations of spin-model simulators. In addition, gate-based simulation approaches can incorporate quantum error correction protocols, which may prove essential for fault-tolerant quantum simulation. The demonstrated concepts can also be readily adapted to other physical platforms, ranging from optical, atomic and molecular systems to solid-state devices.

Received 12 October 2010; accepted 4 January 2011.

- Ladd, T. D. *et al.* Quantum computers. *Nature* **464**, 45–53 (2010).
- Kimble, H. J. The quantum internet. *Nature* **453**, 1023–1030 (2008).
- Schoelkopf, R. J. & Girvin, S. M. Wiring up quantum systems. *Nature* **451**, 664–669 (2008).
- Neeley, M. *et al.* Generation of three-qubit entangled states using superconducting phase qubits. *Nature* **467**, 570–573 (2010).
- Saffman, M., Walker, T. G. & Mølmer, K. Quantum information with Rydberg atoms. *Rev. Mod. Phys.* **82**, 2313–2363 (2010).
- Bloch, I., Dalibard, J. & Zwierger, W. Many-body physics with ultracold gases. *Rev. Mod. Phys.* **80**, 885–964 (2008).
- O'Brien, J. L. Optical quantum computing. *Science* **318**, 1567–1570 (2007).
- Jones, J. A. Quantum computing with NMR. Preprint at (<http://arXiv.org/abs/1011.1382>) (2010).
- Clarke, J. & Wilhelm, F. K. Superconducting quantum bits. *Nature* **453**, 1031–1042 (2008).
- Hanson, R., Kouwenhoven, L. P., Petta, J. R., Tarucha, S. & Vandersypen, L. M. K. Spins in few-electron quantum dots. *Rev. Mod. Phys.* **79**, 1217–1265 (2007).
- Wrachtrup, J. & Jelezko, F. Processing quantum information in diamond. *J. Phys. Condens. Matter* **18**, S807–S824 (2006).
- Feynman, R. Simulating physics with computers. *Int. J. Theor. Phys.* **21**, 467–488 (1982).
- Lloyd, S. Universal quantum simulators. *Science* **273**, 1073–1078 (1996).
- Buluta, I. & Nori, F. Quantum simulators. *Science* **326**, 108–111 (2009).
- Myatt, C. J. *et al.* Decoherence of quantum superpositions through coupling to engineered reservoirs. *Nature* **403**, 269–273 (2000).
- Viola, L. *et al.* Experimental realization of noiseless subsystems for quantum information processing. *Science* **293**, 2059–2063 (2001).
- Deléglise, S. *et al.* Reconstruction of nonclassical cavity field states with snapshots of their decoherence. *Nature* **455**, 510–514 (2008).

- Barreiro, J. T. *et al.* Experimental multiparticle entanglement dynamics induced by decoherence. *Nature Phys.* **6**, 943–946 (2010); published online 26 September 2010.
- Krauter, H. *et al.* Entanglement generated by dissipation. Preprint at (<http://arXiv.org/abs/1006.4344>) (2010).
- Diehl, S. *et al.* Quantum states and phases in driven open quantum systems with cold atoms. *Nature Phys.* **4**, 878–883 (2008).
- Cho, J., Bose, S. & Kim, M. S. Optical pumping into many-body entanglement. *Phys. Rev. Lett.* **106**, 020504 (2011).
- Verstraete, F., Wolf, M. M. & Cirac, J. I. Quantum computation and quantum-state engineering driven by dissipation. *Nature Phys.* **5**, 633–636 (2009).
- Pastawski, F., Clemente, L. & Cirac, J. I. Quantum memories based on engineered dissipation. Preprint at (<http://arXiv.org/abs/1010.2901>) (2010).
- Goldstein, G. *et al.* Environment-assisted precision measurement. Preprint at (<http://arXiv.org/abs/1001.0089>) (2010).
- Lloyd, S. & Viola, L. Engineering quantum dynamics. *Phys. Rev. A* **65**, 010101 (2001).
- Häffner, H., Roos, C. F. & Blatt, R. Quantum computing with trapped ions. *Phys. Rep.* **469**, 155–203 (2008).
- Home, J. P. *et al.* Complete methods set for scalable ion trap quantum information processing. *Science* **325**, 1227–1230 (2009).
- Weimer, H., Müller, M., Lesanovsky, I., Zoller, P. & Büchler, H. P. A Rydberg quantum simulator. *Nature Phys.* **6**, 382–388 (2010).
- Bacon, D. *et al.* Universal simulation of Markovian quantum dynamics. *Phys. Rev. A* **64**, 062302 (2001).
- Kitaev, A. Y. Fault-tolerant quantum computation by anyons. *Ann. Phys.* **303**, 2–30 (2003).
- Nielsen, M. A. & Chuang, I. L. *Quantum Computation and Quantum Information* (Cambridge Univ. Press, 2000).
- Steane, A. M. Efficient fault-tolerant quantum computing. *Nature* **399**, 124–126 (1999).
- Dür, W., Bremner, M. J. & Briegel, H. J. Quantum simulation of interacting high-dimensional systems: the influence of noise. *Phys. Rev. A* **78**, 052325 (2008).
- Wiseman, H. M. & Milburn, G. J. *Quantum Measurement and Control* (Cambridge Univ. Press, 2009).
- Schmidt-Kaler, F. *et al.* How to realize a universal quantum gate with trapped ions. *Appl. Phys. B* **77**, 789–796 (2003).
- Mølmer, K. & Sørensen, A. Multiparticle entanglement of hot trapped ions. *Phys. Rev. Lett.* **82**, 1835–1838 (1999).
- Monz, T. *et al.* Coherence of large-scale entanglement. Preprint at (<http://arXiv.org/abs/1009.6126>) (2010).
- Roos, C. F. *et al.* Control and measurement of three-qubit entangled states. *Science* **304**, 1478–1480 (2004).
- Gilchrist, A., Langford, N. K. & Nielsen, M. A. Distance measures to compare real and ideal quantum processes. *Phys. Rev. A* **71**, 062310 (2005).
- Jozsa, R. Fidelity for mixed quantum states. *J. Mod. Opt.* **41**, 2315–2323 (1994).
- Gühne, O. & Seevinck, M. Separability criteria for genuine multiparticle entanglement. *N. J. Phys.* **12**, 053002 (2010).
- Friedenauer, A., Schmitz, H., Glueckert, J., Porras, D. & Schaetz, T. Simulating a quantum magnet with trapped ions. *Nature Phys.* **4**, 757–761 (2008).
- Kim, K. *et al.* Quantum simulation of frustrated Ising spins with trapped ions. *Nature* **465**, 590–593 (2010).
- Porras, D. & Cirac, J. I. Effective quantum spin systems with trapped ions. *Phys. Rev. Lett.* **92**, 207901 (2004).
- Nayak, C., Simon, S. H., Stern, A., Freedman, M. & Das Sarma, S. Non-abelian anyons and topological quantum computation. *Rev. Mod. Phys.* **80**, 1083–1159 (2008).
- Ralph, T. C., Bartlett, S. D., O'Brien, J. L., Pryde, G. J. & Wiseman, H. M. Quantum nondemolition measurements for quantum information. *Phys. Rev. A* **73**, 012113 (2006).
- Riebe, M. *et al.* Deterministic entanglement swapping with an ion-trap quantum computer. *Nature Phys.* **4**, 839–842 (2008).
- Fleming, G. R., Huelga, S. & Plenio, M. (eds) *New J. Phys.* **12** (Focus on quantum effects and noise in biomolecules), (2010).

Supplementary Information is linked to the online version of the paper at www.nature.com/nature.

Acknowledgements We thank K. Hammerer, I. Chuang, and O. Gühne for discussions and T. Northup for critically reading the manuscript. We acknowledge support by the Austrian Science Fund (FOQUS), the European Commission (AQUITE), the Institut für Quanteninformation GmbH, and a Marie Curie International Incoming Fellowship within the 7th European Community Framework Programme.

Author Contributions M.M. and J.T.B. developed the research, based on theoretical ideas proposed originally by P.Z.; J.T.B., P.S. and D.N. performed the experiments; J.T.B., P.S. and T.M. analysed the data; P.S., J.T.B., D.N., T.M., M.C., M.H. and R.B. contributed to the experimental set-up; M.M., J.T.B. and P.Z. wrote the manuscript, with revisions provided by C.F.R.; all authors contributed to the discussion of the results and manuscript.

Author Information Reprints and permissions information is available at www.nature.com/reprints. The authors declare no competing financial interests. Readers are welcome to comment on the online version of this article at www.nature.com/nature. Correspondence and requests for materials should be addressed to P.Z. (Peter.Zoller@uibk.ac.at; for theory) and R.B. (Rainer.Blatt@uibk.ac.at; for experiment).